PCCP

Cite this: *Phys. Chem. Chem. Phys.*, 2011, **13**, 3231–3236

www.rsc.org/pccp

COMMUNICATION

Trajectory-based solution of the nonadiabatic quantum dynamics equations: an on-the-fly approach for molecular dynamics simulations†

Basile F. E. Curchod, Ivano Tavernelli* and Ursula Rothlisberger

Received 15th October 2010, Accepted 23rd December 2010
DOI: 10.1039/c0cp02175j

The non-relativistic quantum dynamics of nuclei and electrons is solved within the framework of quantum hydrodynamics using the adiabatic representation of the electronic states. An on-the-fly trajectory-based nonadiabatic molecular dynamics algorithm is derived, which is also able to capture nuclear quantum effects that are missing in the traditional trajectory surface hopping approach based on the independent trajectory approximation. The use of correlated trajectories produces quantum dynamics, which is in principle exact and computationally very efficient. The method is first tested on a series of model potentials and then applied to study the molecular collision of H with H_2 using on-the-fly TDDFT potential energy surfaces and nonadiabatic coupling vectors.

Ab initio molecular dynamics[1] has led to a large number of theoretical studies of molecules and solids. In the well-established mixed quantum-classical formulation, and thanks to highly efficient electronic structure methods like Kohn–Sham density functional theory (DFT),[2] simulations on molecular systems with up to thousands of atoms are nowadays feasible. Initially restricted to a single adiabatic state within the Born–Oppenheimer approximation, molecular dynamics was recently extended to the nonadiabatic regime[3–7] providing an important tool for the study of photophysical and photochemical processes. One of the most commonly used nonadiabatic molecular dynamics schemes is Tully's fewest switches trajectory surface hopping[8] (TSH) and its extensions to mixed quantum-classical dynamics.[9] In this framework, the nuclear wavepacket is represented by a swarm of *independent* classical trajectories (independent trajectory approximation, ITA) while the nonadiabatic couplings (NACs) induce hops between different electronic states that occur according to a stochastic algorithm. However, the classical approximation for the motion of the nuclei breaks down when interferences,[10] wavepacket bifurcation,[11] (de)coherence or tunneling effects occur during the dynamics.

Laboratory of Computational Chemistry and Biochemistry, Ecole Polytechnique Fédérale de Lausanne, Switzerland. E-mail: ivano.tavernelli@epfl.ch; Fax: +41 21 693 03 28; Tel: +41 21 693 03 28

† Electronic supplementary information (ESI) available. See DOI: 10.1039/c0cp02175j

As an alternative to trajectory-based approaches, quantum dynamics methods use an exact treatment of both electronic and nuclear wavefunctions (see for example ref. 12). However, the applicability of these methods is hampered by their high computational costs, which limit the number of accessible nuclear degrees of freedom. This usually requires fitting of the relevant electronic potential energy surfaces (PESs) prior to propagation. In addition, many alternative schemes have been proposed to describe the dynamics of the nuclear wavefunction, among which semiclassical approaches,[13,14] extended surface hopping,[15,16] quantum-classical Liouville approaches,[10,17] linearized nonadiabatic dynamics (LAND-map),[18] and *ab initio* multiple spawning methods.[19]

In 1999, Wyatt and coworkers have introduced an alternative formulation of quantum dynamics using a trajectory-based solution of the quantum hydrodynamics (Bohmian) equations,[20] called quantum trajectory method (QTM). In this approach, the nuclear wavepacket is split into fluid elements that represent volume elements of configuration space carrying information like amplitude and phase. Each of them is propagated by a Newton-like equation augmented by a quantum potential. The latter provides correlation between the fluid elements and introduces nuclear quantum effects into the dynamics. Following this work, a multisurface QTM scheme has also been proposed,[21–23] which however uses a diabatic representation of the PESs that unfortunately is not suited for an on-the-fly propagation of nuclear trajectories. In addition another formulation of Bohmian dynamics, which uses a complex action, has been developed.[24]

In this Communication, we propose a new scheme combining the advantages of trajectory-based on-the-fly *ab initio* molecular dynamics with those of quantum trajectory methods. In short, using the QTM formalism adapted to the adiabatic picture for the PESs, we obtain an in principle exact solution of the full (electronic and nuclear) time-dependent Schrödinger equation, which is implemented in an on-the-fly nonadiabatic trajectory-based MD scheme. In contrast to TSH, the proposed NonAdiabatic Bohmian DYnamics (NABDY) approach allows for the nonadiabatic transfer of nuclear amplitude among electronic states and for an accurate description of nuclear quantum effects, which are not entirely captured within the ITA.

We start from the non-relativistic time-dependent Schrödinger equation for a molecular system composed of nuclei and electrons,

$$\hat{H}\Psi(\mathbf{r},\mathbf{R},t) = i\hbar\frac{\partial}{\partial t}\Psi(\mathbf{r},\mathbf{R},t), \tag{1}$$

where $\hat{H} = \hat{T}_N + \widehat{\mathscr{H}}_{\mathrm{el}}$ is the molecular time-independent Hamiltonian and $\Psi(\mathbf{r},\mathbf{R},t)$ the total wavefunction of the system under investigation, $\mathbf{r}$ is the collective position vector of all electrons $\{\mathbf{r}_i\}$, and $\mathbf{R}$ the one of the nuclei $\{\mathbf{R}_\gamma\}$. In the language of quantum hydrodynamics, we will refer to a volume element in configuration space with coordinates $\mathbf{R}$ as *fluid element*. To describe the total wavefunction, we can use the *Ansatz* employed in the derivation of Born–Oppenheimer dynamics,

$$\Psi(\mathbf{r},\mathbf{R},t) = \sum_J^{\infty}\Phi_J(\mathbf{r};\mathbf{R})\Omega_J(\mathbf{R},t). \tag{2}$$

$\{\Phi_J(\mathbf{r};\mathbf{R})\}$ describes a complete set of electronic basis functions that are solutions of the time-independent electronic Schrödinger equation, $\widehat{\mathscr{H}}_{\mathrm{el}}(\mathbf{r};\mathbf{R})\Phi_J(\mathbf{r};\mathbf{R}) = E_J^{\mathrm{el}}(\mathbf{R})\Phi_J(\mathbf{r};\mathbf{R})$, and depend parametrically on the nuclear coordinates $\mathbf{R}$. $\{\Omega_J(\mathbf{R};t)\}$ can be seen as the nuclear part of the wavefunction. $E_J^{\mathrm{el}}(\mathbf{R})$ is called the Jth potential energy surface, which is a function of the nuclear coordinates $\mathbf{R}$. If we insert this *Ansatz* for the total wavefunction into the time-dependent Schrödinger equation and multiply from the left by $\Phi_J^*(\mathbf{r};\mathbf{R})$ we get, after integration over $\mathbf{r}$,

$$\begin{aligned} i\hbar\dot{\Omega}_J(\mathbf{R},t) = &-\sum_\gamma\frac{\hbar^2}{2M_\gamma}\nabla_\gamma^2\Omega_J(\mathbf{R},t) + E_J^{\mathrm{el}}(\mathbf{R})\Omega_J(\mathbf{R},t)\\ &+\sum_{\gamma I}\frac{\hbar^2}{2M_\gamma}D_{JI}^{\gamma}(\mathbf{R})\Omega_I(\mathbf{R},t)\\ &-\sum_{\gamma,I\neq J}\frac{\hbar^2}{M_\gamma}\mathbf{d}_{JI}^{\gamma}(\mathbf{R})\nabla_\gamma\Omega_I(\mathbf{R},t), \end{aligned} \tag{3}$$

where $\mathbf{d}_{JI}^{\gamma}(\mathbf{R}) = \int\Phi_J^*(\mathbf{r};\mathbf{R})[\nabla_\gamma\Phi_I(\mathbf{r};\mathbf{R})]d\mathbf{r}$ are the first order nonadiabatic coupling elements and $D_{JI}^{\gamma}(\mathbf{R}) = \int\Phi_J^*(\mathbf{r};\mathbf{R})[\nabla_\gamma^2\Phi_I(\mathbf{r};\mathbf{R})]d\mathbf{r}$ those of second order. $\dot{\Omega}$ denotes the partial time derivative $\frac{\partial\Omega}{\partial t}$. A possible expression for the nuclear wavefunction is its polar representation:

$$\Omega_J(\mathbf{R},t) = A_J(\mathbf{R},t)e^{\frac{i}{\hbar}S_J(\mathbf{R},t)}, \tag{4}$$

where A represents an amplitude and $S/\hbar$ a phase. Inserting this representation in eqn (3) we obtain, after separating real and imaginary parts (in the adiabatic representation),

$$\begin{aligned} -\dot{S}_J(\mathbf{R},t) = &\sum_\gamma\frac{1}{2M_\gamma}(\nabla_\gamma S_J(\mathbf{R},t))^2 + E_J^{\mathrm{el}}(\mathbf{R})\\ &-\sum_\gamma\frac{\hbar^2}{2M_\gamma}\frac{\nabla_\gamma^2 A_J(\mathbf{R},t)}{A_J(\mathbf{R},t)}\\ &+\sum_{\gamma I}\frac{\hbar^2}{2M_\gamma}D_{JI}^{\gamma}(\mathbf{R})\frac{A_I(\mathbf{R},t)}{A_J(\mathbf{R},t)}\Re[e^{i\phi}]\\ &-\sum_{\gamma,I\neq J}\frac{\hbar^2}{M_\gamma}\mathbf{d}_{JI}^{\gamma}(\mathbf{R})\frac{\nabla_\gamma A_I(\mathbf{R},t)}{A_J(\mathbf{R},t)}\Re[e^{i\phi}]\\ &+\sum_{\gamma,I\neq J}\frac{\hbar}{M_\gamma}\mathbf{d}_{JI}^{\gamma}(\mathbf{R})\frac{A_I(\mathbf{R},t)}{A_J(\mathbf{R},t)}\nabla_\gamma S_I(\mathbf{R},t)\Im[e^{i\phi}] \end{aligned} \tag{5}$$

and

$$\begin{aligned} \dot{A}_J(\mathbf{R},t) = &-\sum_\gamma\frac{1}{M_\gamma}\nabla_\gamma A_J(\mathbf{R},t)\nabla_\gamma S_J(\mathbf{R},t)\\ &-\sum_\gamma\frac{1}{2M_\gamma}A_J(\mathbf{R},t)\nabla_\gamma^2 S_J(\mathbf{R},t)\\ &+\sum_{\gamma I}\frac{\hbar}{2M_\gamma}D_{JI}^{\gamma}(\mathbf{R})A_I(\mathbf{R},t)\Im[e^{i\phi}]\\ &-\sum_{\gamma,I\neq J}\frac{\hbar}{M_\gamma}\mathbf{d}_{JI}^{\gamma}(\mathbf{R})\nabla_\gamma A_I(\mathbf{R},t)\Im[e^{i\phi}]\\ &-\sum_{\gamma,I\neq J}\frac{1}{M_\gamma}\mathbf{d}_{JI}^{\gamma}(\mathbf{R})A_I(\mathbf{R},t)\nabla_\gamma S_I(\mathbf{R},t)\Re[e^{i\phi}], \end{aligned} \tag{6}$$

where $\phi = \frac{1}{\hbar}(S_I(\mathbf{R},t) - S_J(\mathbf{R},t))$.

Eqn (5) and (6) correspond to the *exact* Schrödinger equation for a nuclear wavefunction evolving in the potential of the different electronic surfaces determined by the time-independent Schrödinger equation. In contrast to the single surface case or with the diabatic formulation, time evolution of phases and amplitudes involves first and second order coupling elements that mix in contributions from other PESs. In particular, transfer of amplitude from one PES to another becomes possible thanks to the coupling terms, which make however the solution of the set of eqn (5) and (6) more involved.

In the dynamics that emerges, the first equation, eqn (5), is the equivalent of the classical Hamilton–Jacobi (HJ) equation (first two terms) for the action $S(\mathbf{R},t)$, augmented with two additional parts of quantum nature of order $\hbar$ and $\hbar^2$. The 3rd term is the quantum potential $\mathscr{Q}_J(\mathbf{R},t)$ describing all quantum effects on a single PES and introducing nonlocality,[25] and the 4th to 6th terms constitute the nonadiabatic quantum potential $\mathscr{D}_J(\mathbf{R},t)$ describing interstate contributions.

Applying the gradient with respect to the nucleus β on both sides of eqn (5), we get

$$\nabla_\beta \frac{\partial S_J(\mathbf{R},t)}{\partial t} + \sum_\gamma \left(\frac{1}{M_\gamma}\nabla_\gamma S_J(\mathbf{R},t)\cdot\nabla_\gamma\right)\nabla_\beta S_J(\mathbf{R},t) = -\nabla_\beta[E^J_{el}(\mathbf{R}) + \mathcal{Q}_J(\mathbf{R},t) + \mathcal{V}_J(\mathbf{R},t)] \quad (7)$$

After moving to the Lagrangian frame[20] and using the HJ definition of the momenta $\nabla_\beta S_J(\mathbf{R},t) = \mathbf{P}^J_\beta$, we obtain a Newton-like equation of motion

$$M_\beta \frac{d^2\mathbf{R}^J_\beta}{(dt^J)^2} = -\nabla_\beta[E^J_{\mathrm{el}}(\mathbf{R}) + \mathcal{Q}_J(\mathbf{R},t) + \mathcal{V}_J(\mathbf{R},t)] \quad (8)$$

describing the time evolution (trajectory) of the $\mathbf{R}_\beta$ component of a fluid element on state J with collective variable $\mathbf{R}$ ($d/dt^J = \partial/\partial t + \sum_\gamma \nabla_\gamma S_J(\mathbf{R},t)/M_\gamma\cdot\nabla_\gamma$).

The second equation, eqn (6), corresponds to the continuity equation for the density probability (first two terms) on state J, augmented by three nonadiabatic terms describing the amplitude change of state J due to the coupling with the other states. It is important to stress that within NABDY each fluid element of the configuration space is associated to a collective nuclear coordinate $\mathbf{R}(t)$ (that describes its time evolution according to eqn (8)), an amplitude, $A_J(\mathbf{R},t)$, and a phase, $S_J(\mathbf{R},t)/\hbar$, which determine the quantum potential and the nonadiabatic coupling terms between the states.

A simplified implementation of this coupled set of equations (eqn (5) and (6)) was first proposed by Tully[8] and relies on the ITA. Within this approximation, the nuclear wavepacket propagation is replaced by the time evolution of a set of independent trajectories evolving according to the classical HJ equation (with $\mathcal{Q}_J(\mathbf{R},t) = \mathcal{V}_J(\mathbf{R},t) = 0$ in eqn (5)). This approximation implies that nuclear quantum effects, such as nuclear-nuclear correlation, (de)coherence, interference, and tunneling are neglected. Furthermore, in TSH the density of the nuclear wavepacket is replaced by a density of classical trajectories and the transfer of amplitude by stochastic hops of trajectories among states.

In the NABDY approach, the dynamics associated with eqn (5) and (6) is computed in the following steps: (i) Assign amplitudes and momenta ($\nabla_{\mathbf{R}} S_J(\mathbf{R},t=0)$) to a homogeneous distribution of fluid elements. In contrast to TSH, NABDY trajectories are now carrying quantum information (amplitude and phase) of the nuclear wavefunction, and therefore a faster convergence with respect to the number of trajectories can be expected. (ii) Time propagation of the amplitudes ($A_J(\mathbf{R},t)$) associated to each fluid element according to eqn (6). This implies transfer of amplitude between fluid elements belonging to the same state and between fluid elements on different states. Fluid elements associated to a yet non-populated state are required and generated when the total transferred amplitude (from all other states) exceeds a given threshold ε.‡ (iii) The fluid elements evolve in time according to eqn (5) and (8), producing a swarm of correlated trajectories on each state. The propagation is driven by forces that include the gradient of the quantum potentials $\mathcal{Q}_J(\mathbf{R},t)$ and $\mathcal{V}_J(\mathbf{R},t)$. In NABDY, all fluid elements remain correlated (points ii and iii), which corresponds to a complete relaxation of the ITA approximation implicit in TSH. As an advantage, we obtain a trajectory-based non-adiabatic MD scheme that includes the description of nuclear quantum effects like tunneling, (de)coherence and interferences (see ESI).

Numerically, the NABDY scheme can be directly implemented in any molecular dynamics package, where electronic state energies $E^J_{\mathrm{el}}(\mathbf{R})$ and nonadiabatic couplings $\mathbf{d}^\gamma_{IJ}(\mathbf{R})$ and $D^\gamma_{IJ}(\mathbf{R})$ are computed *on-the-fly* at the desired level of theory (here we use DFT and time-dependent DFT (TDDFT) for the potential energy surfaces and the couplings $\mathbf{d}^\gamma_{IJ}(\mathbf{R})$, and we neglect $D^\gamma_{IJ}(\mathbf{R})$ (see Computational Details)). It is worth mentioning that as a consequence of the correlated propagation of all fluid elements, this scheme requires the simultaneous advancement of all representative trajectories, which however does not constitute a computational overhead compared to TSH on parallel architectures. The accuracy of the NABDY scheme was assessed by direct comparison with exact wavepacket propagation results on Tully model system 1.[8] In this case, we obtained an average deviation of the population of state 2 smaller than 0.6% for momenta between 16 and 22 a.u. (while the TSH average error amounts to 1.6%). We present here two test applications of NABDY.

In the first example, we test the effect of quantum interferences on the wavepacket dynamics by means of a double well potential based on Tully's model I depicted in the inset of Fig. 1. Overall, there is a good agreement between TSH, NABDY and the exact propagation scheme§ in the first part of the dynamics (see Fig. 1, $t < 1250$ a.u.). However, the interaction between the wavepackets on the two states (in the region $5 < x < 15$ a.u.) is not fully captured by TSH because

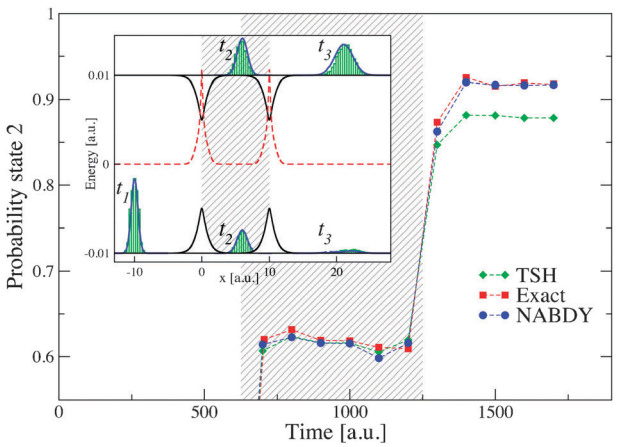

Fig. 1 Population dynamics in a double well potential. We used 3112 trajectories for TSH, 314 for NABDY dynamics, and 8192 grid points for the exact propagation scheme (the initial momentum of the wavepacket, k, is set to 32 a.u. in all cases, reflection of the wavepacket is negligible). Inset: PESs (black lines) and nonadiabatic coupling strength scaled by a factor 1/120 (red dashed line) together with snapshots of the wavepackets (probability densities) according to NABDY (blue lines) and TSH dynamics (green bars) computed at $t_1 = 0$, $t_2 = 1000$, $t_3 = 2000$ a.u. Shaded area on the main panel corresponds to the time the wavepackets spend in the region $x \in [0,10]$ (shaded area in the inset).

of the ITA, leading to a small but sizeable deviation (~4%) in the final populations compared to NABDY and the exact dynamics (which agree over the entire simulation within numerical accuracy). The overall shape of the TSH population distributions is nevertheless in good agreement with the NABDY nuclear density probabilities at all times (Fig. 1, inset). To further test the efficiency of NABDY, we progressively modified the slope of the ground state potential energy curve depicted in the inset of Fig. 1 in order to obtain an acceleration of the ground state wavepacket. This allows us to study the effect of the dephasing of the wavepackets on the accuracy of the different nonadiabatic dynamics schemes (NABDY *vs.* TSH dynamics). We observe (see Table 1) that for different overlaps of the two wavepackets, *i.e.* different values of the slope, the amount of population transfer between the two surfaces changes substantially. When compared to the exact propagation, the TSH results show deviations up to 6% while NABDY is always in good agreement within numerical accuracy. Concerning the convergence of NABDY, it is important to mention that we already observed convergence for a much smaller number of trajectories (60) than what is reported in Fig. 1 (312). However, we opted for a more dense swarm of trajectories in order to improve the spatial resolution of the nuclear wavepackets and to obtain a more accurate integration of the final populations.

In the second example, we apply the NABDY approach to the dynamics of a simple molecular system for which a combined on-the-fly solution of the electronic and nuclear Schrödinger equations is required. To this end, we perform on-the-fly NABDY of the collision of H with H_2 using DFT/TDDFT with the LDA functional for the description of the PESs and the nonadiabatic coupling vectors[26–28] as implemented in the plane wave DFT/TDDFT code CPMD.[29] In order to validate our results, we also performed exact propagation and TSH dynamics of the initial wavepacket using the same PESs and nonadiabatic couplings obtained with NABDY. In Fig. 2, we show the results obtained for an initial momentum $k = 75$ a.u. of the colliding H atom along the collision path shown in the inset of Fig. 2. As expected, due to the strong nonadiabatic coupling, we obtain a partial population of the excited state by simple collision without the need of an external radiation field. The amount of transfer depends on the momentum k of the incident H atom, which for $k = 75$ a.u. amounts to 27.9% (exact: 27.8%). The agreement between NABDY and the exact propagation¶ for the amount of population transferred to the upper surface (inset Fig. 2) is very good, while in the case of TSH the transfer occurs at a slightly faster rate. In Fig. 3, we report the potentials $\mathcal{Q}_J$ and $\mathcal{D}_J$ ($J = 1,2$) associated to the wavepacket centered at $d = 1.75$ a.u. These potentials are not acting on the TSH trajectories and are responsible for the rigorous description of the population transfer in NABDY, even though the *ad hoc* stochastic hops in TSH are also able to reproduce final state populations with good accuracy (final deviation ~ 0.6%). It is worth mentioning that the numerical instabilities usually associated with the calculation of the quantum potential ($\mathcal{Q}(\mathbf{R},t)$) in low dimensional models become tractable in the case of molecular systems described in high dimensional phase space. This is mainly due to the ultrafast decay of quantum coherence in multidimensions[30] and in systems coupled to harmonic baths,[31] and also to the fact that photophysical and photochemical processes are mainly non-stationary in the ultrafast time scale regime (1–100 fs).

In this Communication, we have described a novel trajectory-based approach to perform on-the-fly nonadiabatic MD, which goes beyond the ITA and provides an *in principle* exact description of combined quantum electron-nuclear dynamics. Using correlated trajectories, the derived NABDY scheme is able to capture the additional nuclear quantum effects that are missing in the traditional Tully's TSH approach. The NABDY approach combined with on-the-fly calculations of the adiabatic PESs and nonadiabatic couplings is well-suited for the calculation of all nuclear quantum nonadiabatic dynamics effects of medium to large size molecular systems.

The authors thank Giovanni Ciccotti, Jiří Vaníček, Sara Bonella, Tomáš Zimmermann and Jérôme F. Gonthier for their useful comments. COST action CM0702, Swiss NSF grant 200020-130082, and NCCR-MUST are acknowledged for fundings.

Computational details

In order to ensure a proper calculation of the terms coupling different electronic states, the NABDY equations of motion for phases, amplitudes and velocities are propagated in the Arbitrary Lagrangian-Eulerian (ALE) frame,[32] defined as $d/dt^J = \partial/\partial t + \dot{\mathbf{x}}_J \cdot \nabla_\gamma$, where $\dot{\mathbf{x}}_J$ is an arbitrary grid velocity for state J. Depending on the type of grid used and on the parameters chosen, ALE provides an enhanced stabilization of the propagation.[32–35] Fluid elements on each state are first propagated in the Lagrangian frame ($\dot{\mathbf{x}}_J = \nabla_\gamma S_J(\mathbf{R},t)/M_\gamma$) with

Table 1 Population of the excited state after the first and the second nonadiabatic regions for the model system in Fig. 1. The slope imposed to the ground state potential energy curve is given in the first column. Within parenthesis we report the values obtained with TSH using the same number of trajectories as for NABDY.

	Excited state population after:					
	First nonadiabatic event			Second nonadiabatic event		
Slope [Hartree/Bohr]	Exact	NABDY	TSH	Exact	NABDY	TSH
0.0	0.619	0.616	0.616	0.918	0.917	0.879 (0.876)
-2.5×10^{-4}	0.561	0.563	0.557	0.200	0.201	0.186 (0.175)
-5.0×10^{-4}	0.508	0.511	0.510	0.456	0.454	0.469 (0.435)
-7.5×10^{-4}	0.460	0.464	0.468	0.824	0.828	0.797 (0.780)
-1.0×10^{-3}	0.416	0.420	0.412	0.129	0.130	0.190 (0.269)

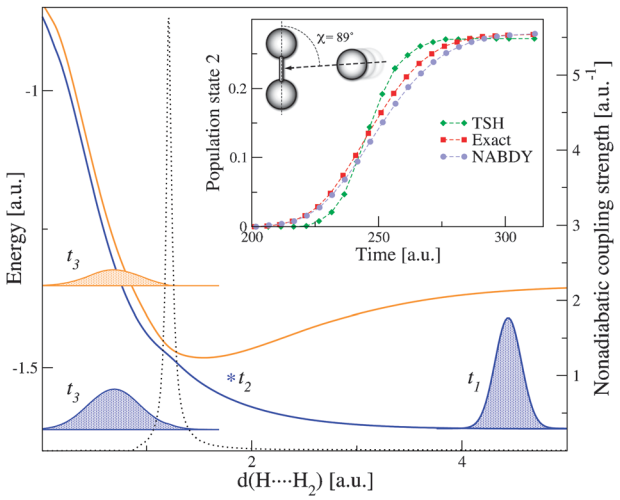

Fig. 2 NABDY applied to the collision of H with H_2 ($\chi = 89°$ and d(H–H) = 1.4 a.u., see figure in the inset). An initial Gaussian wavepacket (wp) is prepared on the ground state ($t_1 = 0$ a.u.) with an initial momentum $k = 75$ a.u. Shown is the probability density of the nuclear wp obtained with 352 trajectories at the initial time (t_1) and after the region of coupling ($t_3 = 300$ a.u.). The displacement of the resulting wps in the vertical direction is arbitrary. Blue: wp on state 1; orange: wp on state 2; black dotted line: nonadiabatic coupling strength. The inset shows the time evolution of the population transfer obtained using the different schemes (TSH: 3112 trajectories).

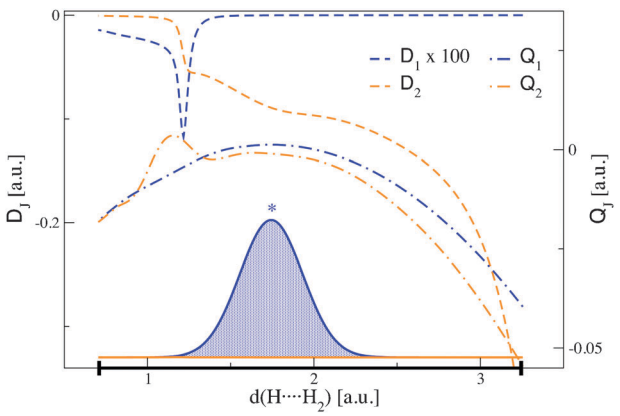

Fig. 3 NABDY applied to the collision of H with H_2 (see Fig. 2, inset). Shown is the quantum potentials ($\mathcal{Q}_J$) and the nonadiabatic quantum potentials ($\mathcal{D}_J$) computed at time t_2 on the support of the nuclear wps (solid black line). At time t_2 the ground state wp is centered at $d = 1.75$ a.u. (asterisk in Fig. 2).

a time step δt. The resulting grids on the different surfaces are then compared and the global minimum and maximum are determined. A regular grid is then created between these two points (conserving the number of fluid elements) and used for both states. The grid velocity is computed according to $\dot{\mathbf{x}}^i_J = (\mathbf{x}^i_J(t + \delta t) - \mathbf{x}^i_J(t))/\delta t$, where i describes each fluid elements and δt represents the time step. The NABDY equations are then propagated in the ALE frame to match exactly the selected grid. Even if derivatives can be obtained with a finite differences scheme, the moving least square (MLS) method[25] is preferred for stability reasons.

NACVs and potential energy surfaces are obtained from DFT and TDDFT calculations using the LDA functional, an energy cutoff of 70 Ry and a cubic box of 20 Bohrs within the plane wave code CPMD. The accuracy of these choices for the H + H_2 system has already been assessed in ref. 26. It is important to note that second order NACs are generally difficult to compute but can be approximated in the case of two level systems.[36] Even though these couplings are small, neglecting them often affects the norm conservation of the nuclear wavepacket. However, due to the low dimensionality of our applications, we have decided not to include the contribution of the $D^{(2)}_{IJ}(\mathbf{R})$ terms in our calculations. The effects are small variations of the norm that never exceed 1% in all simulations. We are currently working on the implementation of the second order nonadiabatic terms within TDDFT. This step is required in the prospective to move towards the study of the dynamics of larger systems for which the neglect of second order NACs can lead to important errors in norm conservation.[37]

References

‡ In all examples studied, we obtained convergence of the NABDY results for ε of the order of 10^{-6}.
§ The exact wavepacket propagation was performed in the adiabatic representation using the Fourier propagation method (courtesy of J. Vaníček and T. Zimmermann).
¶ The exact wavepacket propagation is performed on fitted one dimensional TDDFT surfaces produced by the unconstrained NABDY dynamics.

1 D. Marx and J. Hutter, in *Modern Methods and Algorithms of Quantum Chemistry*, ed. J. Grotendorst, Forschungszentrum Juelich, 2000, vol. 1, p. 301.
2 W. Kohn and L. J. Sham, *Phys. Rev.*, 1965, **140**, A1133.
3 N. L. Doltsinis and D. Marx, *Phys. Rev. Lett.*, 2002, **88**, 166402.
4 C. F. Craig, W. R. Duncan and O. V. Prezhdo, *Phys. Rev. Lett.*, 2005, **95**, 163001.
5 E. Tapavicza, I. Tavernelli and U. Rothlisberger, *Phys. Rev. Lett.*, 2007, **98**, 023001.
6 E. Tapavicza, I. Tavernelli, U. Rothlisberger, C. Filippi and M. E. Casida, *J. Chem. Phys.*, 2008, **129**, 124108.
7 I. Tavernelli, B. F. E. Curchod and U. Rothlisberger, *Phys. Rev. A*, 2010, **81**, 052508.
8 J. C. Tully, *J. Chem. Phys.*, 1990, **93**, 1061.
9 S. Nielsen, R. Kapral and G. Ciccotti, *J. Chem. Phys.*, 2000, **112**, 6543.
10 I. Horenko, C. Salzmann, B. Schmidt and C. Schutte, *J. Chem. Phys.*, 2002, **117**, 11075.
11 Y. Arasaki, K. Takatsuka, K. Wang and V. McKoy, *Phys. Rev. Lett.*, 2003, **90**, 248303.
12 H. D. Meyer, U. Manthe and L. S. Cederbaum, *Chem. Phys. Lett.*, 1990, **165**, 73.
13 M. F. Herman, *J. Chem. Phys.*, 1984, **81**, 754.
14 X. Sun and W. H. Miller, *J. Chem. Phys.*, 1997, **106**, 6346.
15 D. F. Coker and L. Xiao, *J. Chem. Phys.*, 1995, **102**, 496.
16 E. R. Bittner and P. J. Rossky, *J. Chem. Phys.*, 1995, **103**, 8130.
17 A. Donoso and C. C. Martens, *J. Phys. Chem. A*, 1998, **102**, 4291.
18 S. Bonella and D. F. Coker, *J. Chem. Phys.*, 2005, **122**, 194102.
19 M. Ben-Nun and T. J. Martinez, *J. Chem. Phys.*, 1998, **108**, 7244.
20 C. L. Lopreore and R. E. Wyatt, *Phys. Rev. Lett.*, 1999, **82**, 5190.
21 R. E. Wyatt, C. L. Lopreore and G. Parlant, *J. Chem. Phys.*, 2001, **114**, 5113.
22 C. L. Lopreore and R. E. Wyatt, *J. Chem. Phys.*, 2002, **116**, 1228.
23 B. Poirier and G. Parlant, *J. Phys. Chem. A*, 2007, **111**, 10400.
24 Y. Goldfarb, I. Degani and D. J. Tannor, *J. Chem. Phys.*, 2006, **125**, 231103.
25 R. E. Wyatt, *Quantum dynamics with trajectories: Introduction to quantum hydrodynamics*, Interdisciplinary applied mathematics, 2005.
26 I. Tavernelli, E. Tapavicza and U. Rothlisberger, *J. Chem. Phys.*, 2009, **130**, 124107.

27 I. Tavernelli, B. F. E. Curchod and U. Rothlisberger, *J. Chem. Phys.*, 2009, **131**, 196101.
28 I. Tavernelli, B. F. E. Curchod, A. Laktionov and U. Rothlisberger, *J. Chem. Phys.*, 2010, **133**, 194104.
29 *CPMD*, Copyright IBM Corp 1990–2001, Copyright MPI für Festkörperforschung Stuttgart, 1997–2001.
30 G. Stock, *J. Chem. Phys.*, 1995, **103**, 10015.
31 R. E. Wyatt and K. Na, *Phys. Scr.*, 2003, **67**, 169.
32 B. K. Kendrick, *J. Chem. Phys.*, 2003, **119**, 5805.
33 R. E. Wyatt and E. R. Bittner, *J. Chem. Phys.*, 2000, **113**, 8898.
34 R. E. Wyatt, *J. Chem. Phys.*, 2002, **117**, 9569.
35 K. H. Hughes and R. E. Wyatt, *Chem. Phys. Lett.*, 2002, **366**, 336.
36 A. Hofmann and R. de Vivie-Riedle, *Chem. Phys. Lett.*, 2001, **346**, 299.
37 S. Ronen, D. Nachtigallová, B. Schmidt and P. Jungwirth, *Phys. Rev. Lett.*, 2004, **93**, 048301.

